Please cite this article in press as: Hu et al., H2A.Z Facilitates Access of Active and Repressive Complexes to Chromatin in Embryonic Stem Cell Self-Renewal and Differentiation, Cell Stem Cell (2013), http://dx.doi.org/10.1016/j.stem.2012.11.003

Cell Stem Cell
Article

H2A.Z Facilitates Access of Active and Repressive Complexes to Chromatin in Embryonic Stem Cell Self-Renewal and Differentiation

Gangqing Hu,[1,6] Kairong Cui,[1,6] Daniel Northrup,[1,6] Chengyu Liu,[2] Chaochen Wang,[3] Qingsong Tang,[1] Kai Ge,[3] David Levens,[4] Colyn Crane-Robinson,[5] and Keji Zhao[1,*]
[1]Systems Biology Center, National Heart, Lung, and Blood Institute
[2]Transgenic Mouse Facility, National Heart, Lung, and Blood Institute
[3]Laboratory of Endocrinology and Receptor Biology, National Institute of Diabetes and Digestive and Kidney Diseases
[4]Laboratory of Pathology, National Cancer Institute
National Institutes of Health, Bethesda, MD 20892, USA
[5]Biophysics Laboratories, St. Michael's Building, University of Portsmouth, Portsmouth PO1 2DT, UK
[6]These authors contributed equally to this work
*Correspondence: zhaok@nhlbi.nih.gov
http://dx.doi.org/10.1016/j.stem.2012.11.003

SUMMARY

Chromatin modifications have been implicated in the self-renewal and differentiation of embryonic stem cells (ESCs). However, the function of histone variant H2A.Z in ESCs remains unclear. We show that H2A.Z is highly enriched at promoters and enhancers and is required for both efficient self-renewal and differentiation of murine ESCs. H2A.Z deposition leads to an abnormal nucleosome structure, decreased nucleosome occupancy, and increased chromatin accessibility. In self-renewing ESCs, knockdown of H2A.Z compromises OCT4 binding to its target genes and leads to decreased binding of MLL complexes to active genes and of PRC2 complex to repressed genes. During differentiation of ESCs, inhibition of H2A.Z also compromises RA-induced RARα binding, activation of differentiation markers, and the repression of pluripotency genes. We propose that H2A.Z mediates such contrasting activities by acting as a general facilitator that generates access for a variety of complexes, both activating and repressive.

INTRODUCTION

Recent studies have revealed that eukaryotic genomes are characterized by a large number of histone modification patterns and chromatin states, which are dependent on the differentiation status of cells (Ernst et al., 2011). In all cell types, inactive genes are mainly associated with the repressive H3K27me3 mark, while nucleosomes at active promoters and enhancers are often associated with multiple different modifications including a variety of histone methylations, histone acetylation, and deposition of histone variants (Barski et al., 2007; Bruce et al., 2005; Goldberg et al., 2010; Guenther et al., 2007; Heintzman et al., 2007; Jin et al., 2009; Kim et al., 2005; Mikkelsen et al., 2007; Wang et al., 2008).

The histone variant H2A.Z is conserved from yeast to humans and is implicated in multiple nuclear processes, including genome integrity, X chromosome inactivation, DNA repair, and transcriptional regulation (Zlatanova and Thakar, 2008), by impacting chromatin structure (Goldman et al., 2010; Jin and Felsenfeld, 2007; Kim et al., 2009; Thambirajah et al., 2006; Tolstorukov et al., 2009; Fan et al., 2002, 2004). H2A.Z is localized to promoters of active genes in various systems, suggesting a positive role in gene regulation (Barski et al., 2007; Bruce et al., 2005; Conerly et al., 2010; Cui et al., 2009; Dryhurst et al., 2009; Hardy et al., 2009; Leach et al., 2000; Ren and Gorovsky, 2001; Valdés-Mora et al., 2012; Zilberman et al., 2008). In contrast, H2A.Z was first described as a component of pericentric heterochromatin (Rangasamy et al., 2003). Particularly in embryonic stem cells (ESCs), H2A.Z was reported to localize exclusively at polycomb complex target genes and mediate the targeting of PRC2 and repression of these genes, but not be required for the self-renewal of ESCs (Creyghton et al., 2008).

To clarify the function of H2A.Z in ESCs and to understand how H2A.Z functions together with other mechanisms of chromatin modification such as histone methylation by the MLL family of histone H3K4 methyltransferases, we investigated the genomic distribution profiles of H2A.Z, acetylated H2A.Z, histone modifications H3K4me3 and H3K27me3, and RbBP5 (a core subunit of the MLL complexes) in mouse ESCs using ChIP-seq and tested the activities of H2A.Z in ESC self-renewal and differentiation. Our data indicate that H2A.Z is enriched at active enhancers and promoters and facilitates chromatin accessibility to allow binding of a variety of active and repressive complexes required for ESC self-renewal and differentiation.

RESULTS

H2A.Z Is Highly Enriched at Active Promoters and Enhancers in ESCs

We profiled the genome-wide distribution of H2A.Z in mouse ESCs with ChIP-seq using antibodies that recognize acetylated H2A.Z (hereafter acH2A.Z) (Bruce et al., 2005) and H2A.Z

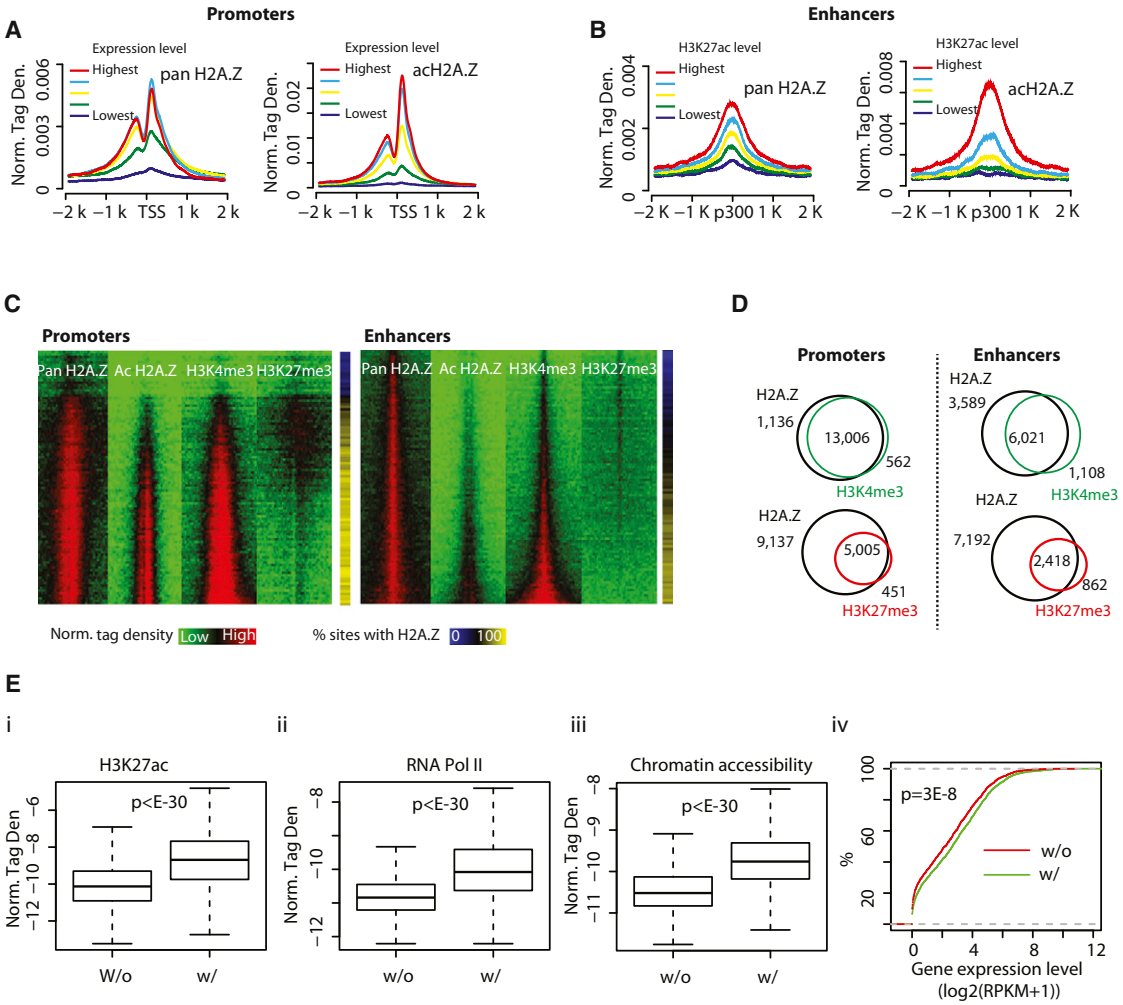

Figure 1. H2A.Z Marks Open Chromatin and Is Colocalized with H3K4me3 at Promoters and Enhancers

(A) Left panel: relationship of normalized, averaged tag density of pan H2A.Z across TSSs to expression levels. All nonlocally redundant genes were sorted into five equal-sized groups according to their mRNA expression values (RPKM). Right panel: a similar plot for acH2A.Z across TSSs.

(B) Left panel: normalized tag density of pan H2A.Z across intergenic p300 binding sites, sorted into five equal-sized groups by their H3K27ac level. Right panel: a similar plot for acH2A.Z across intergenic p300 binding sites.

(C) Heatmaps of pan H2A.Z, acH2A.Z, and histone modifications H3K4me3 and H3K27me3 in promoter regions (left panel) and enhancer regions (right panel), ±3 kb around TSS and intergenic p300 binding sites, respectively (see Supplemental Experimental Procedures for details). The rightmost bars indicate the percentage of promoters and enhancers that showed enrichment of pan H2A.Z for each bin.

(D) Venn diagrams for promoters (left panel) and enhancers (right panel) occupied by pan H2A.Z and either H3K4me3 (green) or H3K27me3 (red).

(E) Enhancers associated with both H2A.Z and H3K4me3 are more likely to be active. Boxplots of (i) H3K27ac ChIP-seq tag densities, (ii) RNA Pol II ChIP-seq tag densities, and (iii) BNase-seq tag densities, which measure chromatin accessibility around intergenic p300 binding sites that are bound by H2A.Z (±2.5 kb; H2A.Z bound enhancers). The binding sites are separated into two groups based on presence (w/) or absence (w/o) of H3K4me3 islands. The top and bottom of the box represent 25th and 75th percentile, respectively. The upper whisker represents the smaller of the maximum and upper quartile plus 1.5 IQR (interquartile range), while the lower whisker represents the larger of the minimum and lower quartile minus 1.5 IQR. p values were calculated by the t test. (iv) Percent of H2A.Z-bound enhancers (y axis) whose target genes exhibit lower expression than the value specified by the x axis. The potential target of an H2A.Z-bound enhancer is defined by its nearest gene within 100 kb. A line shifted to the left side indicates a globally lower level of expression. The p value was calculated by the Kolmogorov-Smirnov test. See also Figure S1.

irrespective of its state of acetylation (hereafter pan H2A.Z). This led to the identification of 51,536 islands of pan H2A.Z and 32,248 islands of acH2A.Z using the SICER program (Zang et al., 2009). The islands are highly enriched at promoter and enhancer regions (Figures S1A–S1C). A positive correlation between gene expression levels and the enrichment of pan H2A.Z and acH2A.Z surrounding TSSs was found (Figure 1A). The percentage of H2A.Z acetylation increased with gene expression level (Figure S1D). Interestingly, even at the promoters of genes without detectable levels of expression, two-thirds of the associated H2A.Z islands were acetylated (Figure S1D). We next examined the pan H2A.Z and acH2A.Z levels at enhancers, defined by intergenic p300 sites, and grouped by the levels of H3K27ac, a marker of active enhancers

(Hawkins et al., 2011; Creyghton et al., 2010; Rada-Iglesias et al., 2011). The average profiles of pan H2A.Z and acH2A.Z tag density were positively correlated with the level of H3K27ac (Figure 1B). Again, the percentage of H2A.Z acetylation reached close to 100% for enhancers having the highest levels of H3K27ac (Figure S1E).

H2A.Z and H3K4me3 Are Colocalized at Both Promoters and Enhancers

To test whether H2A.Z is positively correlated with active or repressive histone modifications in ESCs, we compared our H2A.Z profiles with H3K4me3 and H3K27me3 profiles determined by others (Meissner et al., 2008; Mikkelsen et al., 2007) using a clustering analysis of all promoters ranked from lowest to highest gene expression levels in ESCs (Figure 1C, left panel). Both pan H2A.Z and acH2A.Z were highly correlated with H3K4me3 at active promoters. Globally, 92% of the H2A.Z-bound promoters were associated with H3K4me3 (Figure 1D, left panel). Examination of the distribution of H2A.Z, H3K4me3, and H3K27me3 at the *Hoxa10* promoter indicated a better spatial correlation between H2A.Z and H3K4me3 than with H3K27me3 (Figure S1F). Global analysis revealed that the spatial distribution of H2A.Z was highly correlated with H3K4me3 but less so with H3K27me3 (Figure S1G).

While enhancers are generally associated with H3K4me1 (Heintzman et al., 2007), active enhancers are also marked by H3K4me2 (He et al., 2010; Pekowska et al., 2010; Wang et al., 2008), H3K4me3 (Pekowska et al., 2011; Wang et al., 2008), H3K27ac (Creyghton et al., 2010; Wang et al., 2008), and H3K9acK14ac (Roh et al., 2005, 2007), and poised enhancers are associated with H3K27me3 (Rada-Iglesias et al., 2011). The positive correlation of H2A.Z with H3K27ac (Figure 1B) suggested that it may also be colocalized with H3K4me3 at enhancers. We therefore compared the binding levels of H2A.Z and H3K4me3 modification using a clustering analysis of intergenic p300 binding sites ranked by their H3K27ac levels. We found that the pattern of pan H2A.Z distribution paralleled that of H3K4me3 at enhancers as well as promoters (Figure 1C, right panel). Only a minor fraction of the enhancers were associated with both H2A.Z and H3K27me3; these were bivalent enhancers as indicated by the coexistence of H3K4me3 and H3K27me3. The acH2A.Z distribution showed an inverse pattern from that of H3K27me3, suggesting that it is mainly located in active enhancers. In total, among the 9,610 H2A.Z-bound enhancers, 63% were also associated with H3K4me3 (Figure 1D, right panel). The Pearson coefficient analysis indicated that H2A.Z was much better correlated with H3K4me3 than with H3K27me3 at enhancers (Figure S1H). Using H3K4me1 as an enhancer marker revealed a similar correlation between H2A.Z and H3K4me3 at enhancers (Figures S1I and S1J). These data indicate that H2A.Z is colocalized with H3K4me3 at active regulatory regions of transcription in ESCs. We further analyzed how H2A.Z-containing nucleosomes are associated with histone acetylation and methylation at a resolution of individual nucleosomes and found that H2A.Z-containing nucleosomes are more frequently modified by H3K4me3 than H3K27me3 and prefer H3K27ac to H3K9ac in the genome (Figure S1K).

Enhancers Associated with Both H2A.Z and H3K4me3 Are More Likely to Be Active

Among the H2A.Z-bound enhancers, 63% are also associated with H3K4me3. We found that the H2A.Z-bound enhancers with H3K4me3 are associated with higher levels of H3K27ac and RNA Pol II and have higher chromatin accessibility than enhancers lacking H3K4me3 (Figure 1Ei–1Eiii). The expression levels of putative target genes (the nearest gene within ±100 kb) for H2A.Z-bound enhancers with H3K4me3 are significantly higher than those without H3K4me3 (Figure 1Eiv), suggesting that enhancers with both H2A.Z and H3K4me3 are more likely to be active. The top gene ontology (GO) terms of target genes of H3K4me3-positive H2A.Z-containing enhancers are mainly associated with housekeeping functions such as the regulation of cellular, metabolic, and biosynthetic processes (Figure S1Li), while those for H3K4me3-negative enhancers show preference toward system development and cell differentiation (Figure S1Lii).

H2A.Z Promotes H3K4me3 and H3K27me3 by Facilitating the Binding of the MLL and PRC2 Complexes

To test if H2A.Z facilitates histone methylation, we knocked down H2A.Z using shRNAs (Figure S2A) and measured global changes in H3K4me3 and H3K27me3 by ChIP-seq. We first quantified the histone modifications in defined regions (promoters, enhancers) and plotted the fold change (FC) of each histone modification between control and H2A.Z knockdown cells versus the average level of the modification (termed MA analyses hereafter). At promoters we found that H3K4me3 modification was only modestly affected by knocking down H2A.Z, whereas a stronger effect was detected with the H3K27me3 modification (Figure S2B). At enhancers, H2A.Z knockdown resulted in a substantial decrease in both the H3K4me3 and H3K27me3 signals (Figure 2A). It is interesting to note that greater decreases in H3K4me3 were detected at weaker sites than at stronger sites (Figure 2A, left panel).

H3K4me3 and H3K27me3 modifications are generated by the MLL and PRC2 complexes, respectively (Schuettengruber et al., 2007). Our data showed that RbBP5, a core subunit of MLL complexes (Cho et al., 2007; Dou et al., 2006), colocalizes with the H3K4me3 and pan/acH2A.Z islands (Figure S2C, upper panels), while SUZ12, a core subunit of the PRC2 complex (Cao and Zhang, 2004), predominantly localizes to the H3K27me3 islands (Figure S2C, lower panels). Consistent with the histone modification changes, both RbBP5 and SUZ12 exhibited substantial decreases in binding to enhancers (Figure 2B) and promoters in the H2A.Z knockdown cells (Figure S2D). Interestingly, H2A.Z knockdown led to greater decreases in RbBP5 binding at enhancers with lower levels of H3K4me3 in contrast to sites with higher levels of H3K4me3 (Figure 2C, left panel), which is consistent with the greater loss of H3K4me3 at enhancers with lower H3K4me3 levels (Figure 2A, left panel). In contrast, SUZ12 binding decreased at all H3K27me3 sites (Figure 2C, right panel).

These results indicate that H2A.Z regulates H3K4me3 and H3K27me3 methylations by facilitating the targeting of the MLL and PRC2 complexes to promoters and particularly to enhancers.

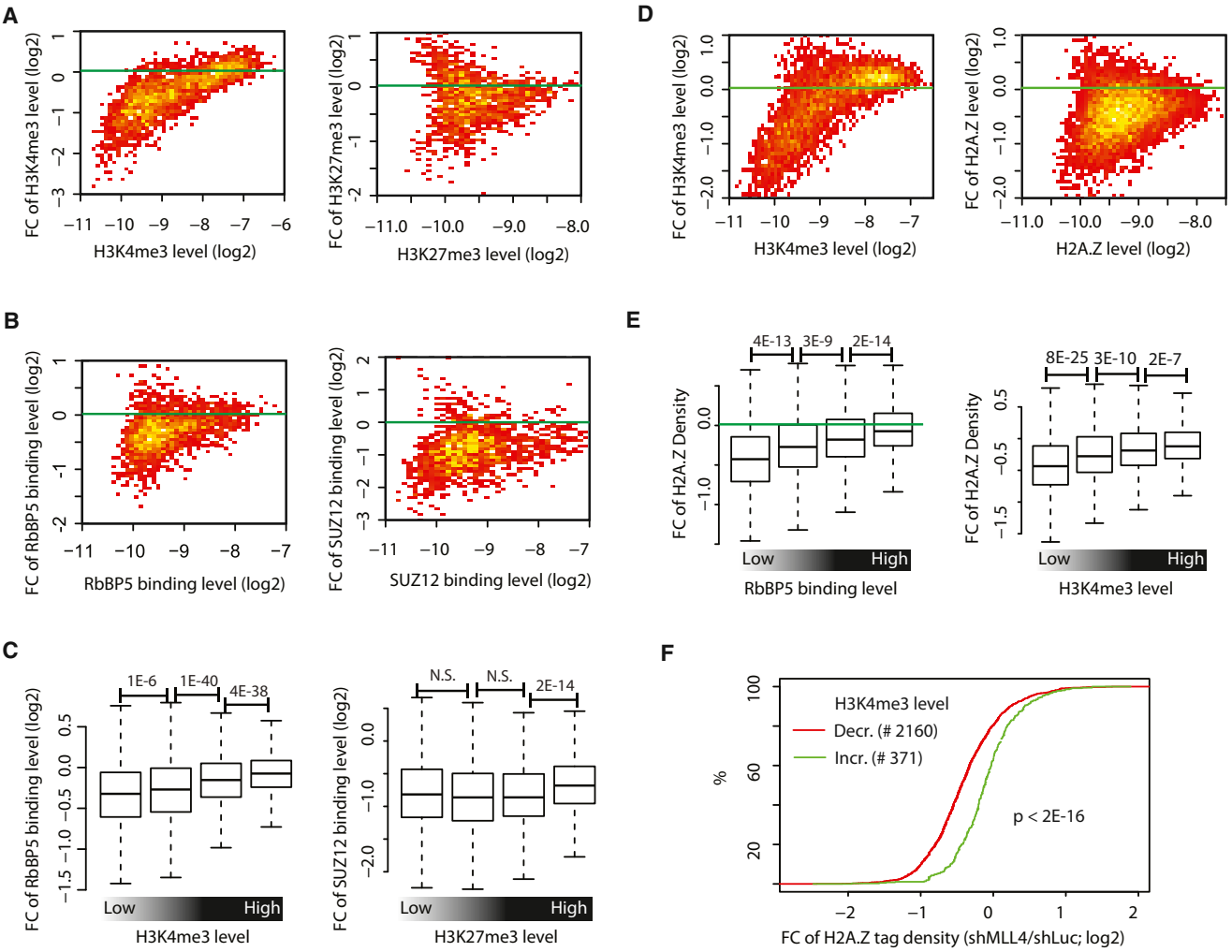

Figure 2. Interregulation of H2A.Z, H3K4me3, and H3K27me3 at Enhancers

(A) MA analysis (see Supplemental Experimental Procedures for details) for H3K4me3 (left panel) and H3K27me3 (right panel) in enhancer regions. The analysis was made from H2A.Z knockdown cells and shLuc control.

(B) MA analysis for RbBP5 (left panel) and Suz12 (right panel) in enhancer regions, as in (A).

(C) Left panel: RbBP5 islands from enhancer regions were sorted into quartiles by the levels of H3K4me3. Shown for each group is a boxplot (see Figure 1E legend for explanation) for the FC of RbBP5 tag density (shH2A.Z/shLuc). Right panel: as left panel, except the calculation was made for SUZ12 and H3K27me3. p values were calculated by the t test.

(D) MA analysis for H3K4me3 (left panel) and H2A.Z (right panel) in enhancer regions. The analysis was made from MLL4 knockdown cells and shLuc control.

(E) Left panel: H2A.Z islands from enhancer regions were sorted into quartiles by the levels of RbBP5 binding. Shown for each group is a boxplot (see Figure 1E legend for explanation) for the FC of RbBP5 tag density (shMLL4/shLuc). Right panel: as left panel, except the calculation was made for H2A.Z and H3K4me3. p values were calculated by the t test.

(F) Empirical cumulative distribution for the FC of H2A.Z ChIP-seq tag density (shMLL4/shLuc) for enhancers that show H3K4me3 decrease by more than 1.5-fold upon MLL4 knockdown (red line). y axis shows the percent of enhancers that exhibit a lower FC of H2A.Z level than the value specified by the x axis. Enhancers that show H3K4me3 increase by more than 1.5-fold are chosen as control (green line). A line shifted to the left means a systematically larger decrease in the H2A.Z levels. p value was calculated by Kolmogorov-Smirnov test. See also Figure S2 and Table S1.

H3K4me3 Promotes H2A.Z Deposition at Enhancers

To test whether H3K4me3 modification influences H2A.Z deposition, we knocked down MLL4, an H3K4 methyltransferase highly expressed in ESCs (Cho et al., 2009) (Figure S2E). Although the expression of MLL4 was decreased by 80%, we did not find detectible changes in overall levels of H3K4me3 by western blotting (data not shown). To determine whether MLL4 nevertheless regulates H3K4 methylation at specific enhancers, we mapped the genome-wide distribution of H3K4me3 in the control and MLL4 knockdown cells and quantified the changes at enhancers by MA analyses. Interestingly, H3K4me3 decreased at a large number of enhancers following MLL4 knockdown, with more severe loss of methylation signals being at enhancers with lower levels of this modification (Figure 2D, left panel). Profiling the distribution of H2A.Z in these cells revealed substantial decreases of H2A.Z at enhancers in

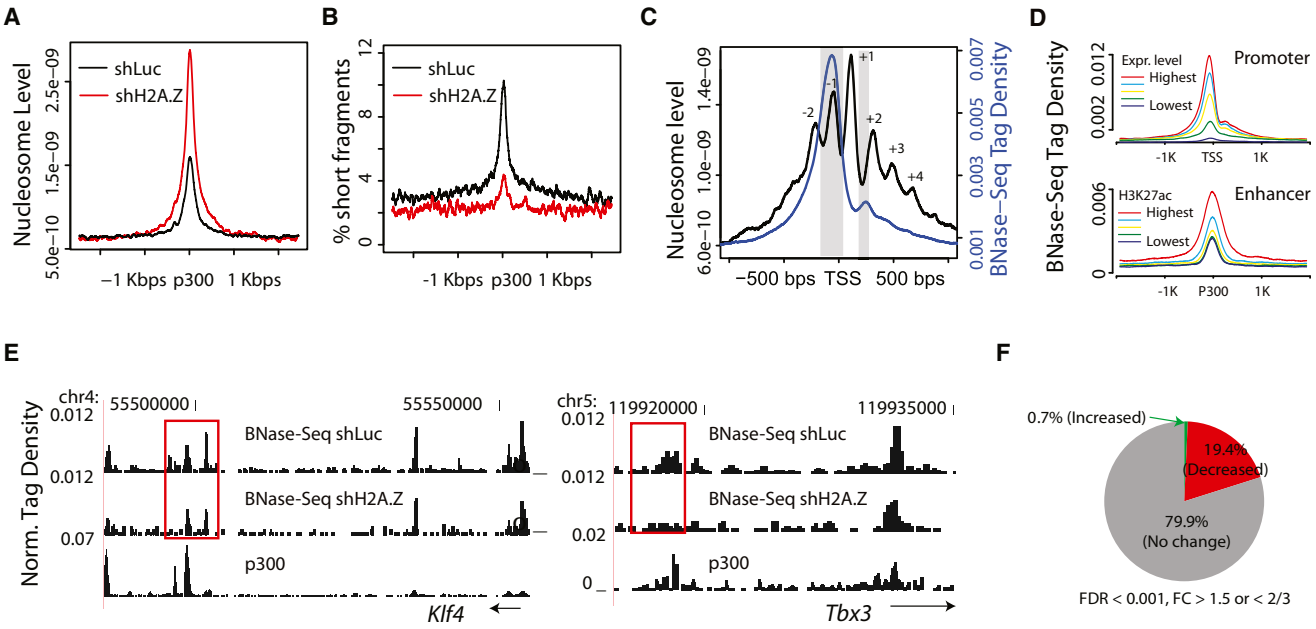

Figure 3. H2A.Z Regulates Nucleosome Organization and Chromatin Accessibility at Enhancers

(A) The nucleosome level at p300-bound enhancers is significantly increased after knockdown of H2A.Z.

(B) Percentage of short fragments (<120 bp) as a function of position relative to the p300 binding site.

(C) Normalized BNase-seq tag density (blue) and nucleosome tag density (black) in regions ±1 kb around TSS. Inferred nucleosome positions are numbered as indicated. The regions immediately upstream of the TSS and the linker region between nucleosomes +1 and +2 that are preferentially digested by Benzonase are highlighted in gray.

(D) Normalized BNase-seq tag densities across TSSs (upper panel) and across intergenic p300 binding sites (lower panel). The TSSs and p300 binding sites were sorted into five equal-sized groups based on gene expression level and H3K27ac level, respectively.

(E) UCSC Genome Browser images for the BNase-seq tag distribution in H2A.Z knockdown and control cells. Potential enhancer regions associated with *Klf4* (left) and *Tbx3* (right) are chosen as examples. p300 genomic regions that show significantly decreased levels of chromatin accessibility following knockdown of H2A.Z are highlighted with red rectangles.

(F) The percentages of hypersensitive sites that show a significant increase in accessibility (green), decrease in accessibility (red), or no change in accessibility (gray) following knockdown of H2A.Z. See also Figure S3.

the MLL4 knockdown cells, particularly at enhancers with lower levels of H2A.Z (Figure 2D, right panel). To directly test how the H2A.Z change is related to the binding of the MLL complex at enhancers, we compared the FC of H2A.Z with RbBP5 binding levels. Interestingly, the analysis revealed greater reductions in H2A.Z deposition in the regions with lower levels of RbBP5 binding after MLL4 knockdown (Figure 2E, left panel), which is consistent with the observation that greater losses of H2A.Z were detected at sites of weaker H3K4 methylations (Figure 2E, right panel). In addition, enhancers that showed decreased levels of H3K4me3 exhibited significantly more loss of H2A.Z deposition than those that showed an increase (Figure 2F), suggesting a causal link between the H3K4me3 change and changes in H2A.Z deposition in the MLL4 knockdown cells.

These results indicate that H3K4me3 modification facilitates the deposition of H2A.Z at enhancers. Furthermore, the results also suggest that higher levels of active histone modifications help to maintain the robustness of chromatin configuration and gene expression. In support of this hypothesis, we found that knockdown of H2A.Z resulted in significantly more genes having changed expression in the poorly methylated group than in the highly methylated group (Figure S2F).

H2A.Z Regulates Chromatin Accessibility

We previously proposed that deposition of histone variants H2A.Z and H3.3 in transcriptional regulatory regions destabilizes nucleosome structure and provides opportunities for the binding of transcription factors (Jin et al., 2009). Another recent report suggested that, in colon cancer cells, H2A.Z is an essential factor for gene reactivation by facilitating nucleosome removal (Yang et al., 2012). To test whether deposition of H2A.Z in ESCs regulates nucleosome occupancy and chromatin accessibility at transcriptional regulatory regions, we determined the global nucleosome distribution in control and H2A.Z knockdown cells using MNase-seq (Schones et al., 2008). Consistent with the previous reports (Hu et al., 2011; Tillo et al., 2010), in control ESs, enhancers are associated with increased nucleosome occupancy relative to neighboring regions (Figure 3A, black line), and H2A.Z knockdown leads to increased nucleosome levels at enhancer sites (Figure 3A, red versus black lines). These data indicate that replacement of H2A.Z with canonical H2A leads to enhanced nucleosome deposition. Thus H2A.Z binding at enhancers destabilizes the local nucleosome structure and facilitates nucleosome removal.

In human T cells, nucleosomes with H2A.Z protect only ~120 bp of DNA from MNase digestion, a fragment shorter

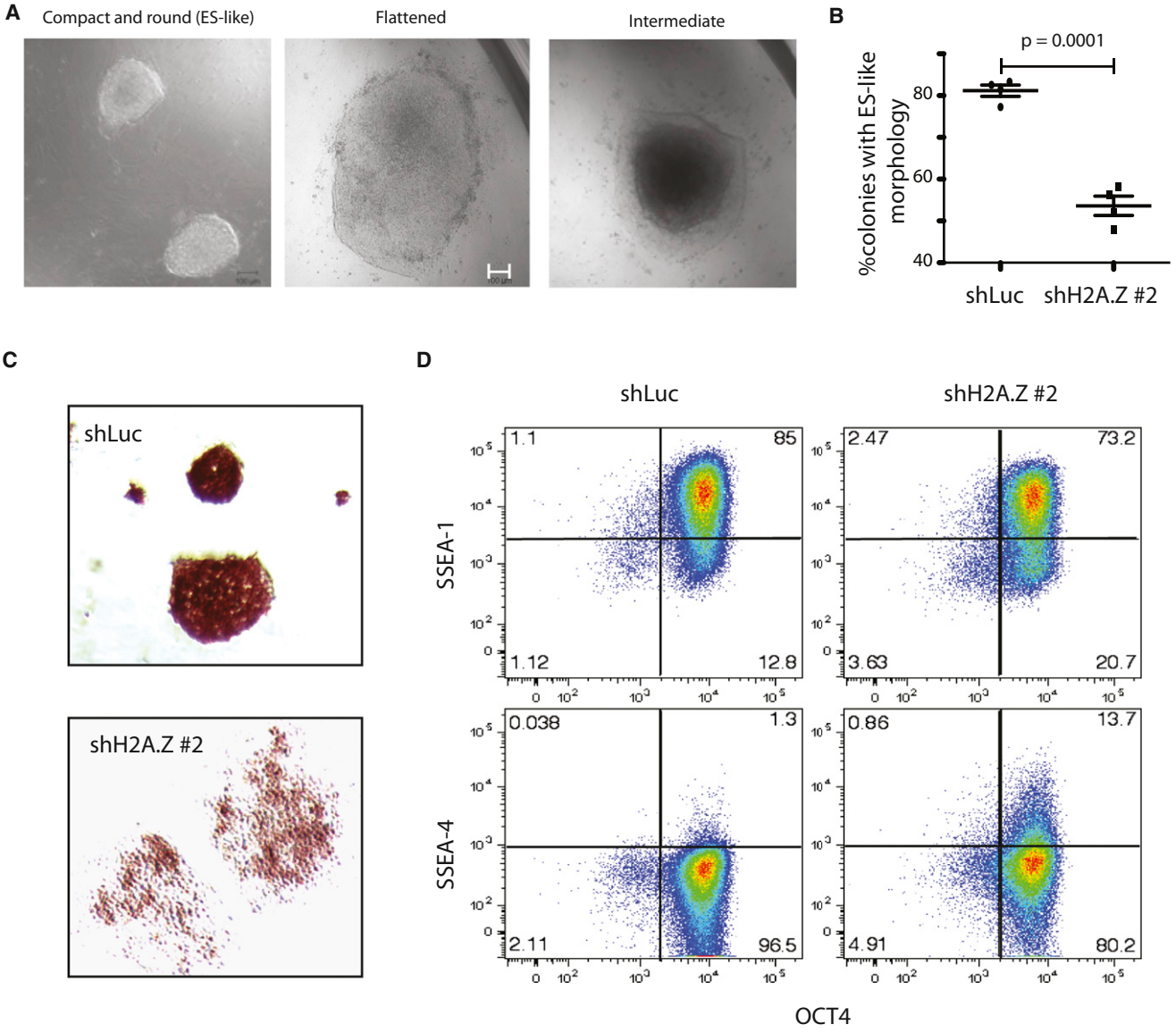

Figure 4. H2A.Z Is Required for ESC Self-Renewal

(A) H2A.Z RNAi ESC colonies are scored by morphology: compact and round (ES-like), flattened, and intermediate. Scale bar, 100 μm.

(B) GFP + ESCs were sorted into a 96-well plate with a murine embryonic fibroblast (MEF) feeder layer. One week later, colonies were scored by morphology. The experiments were carried out for H2A.Z knockdown ESCs and control ESCs side-by-side and were repeated four times. The percentages of colonies that maintain ES-like morphology (compact and round) are represented as mean ± SEM. The p value was calculated by the t test.

(legend continued on next page)

than that given by canonical nucleosomes (Tolstorukov et al., 2009). In ESCs, short DNA fragments (90–120 bp) resulting from MNase digestion were enriched in regions surrounding intergenic p300 binding sites and positively correlated with enhancer activities as measured by the level of H3K27ac (Figure S3A). This is consistent with the hypothesis that nucleosomes are unstable at these regulatory regions. Importantly, knockdown of H2A.Z resulted in a 2- to 3-fold reduction in the density of short fragments surrounding intergenic p300 binding sites (Figure 3B), indicating that H2A.Z deposition contributes to the generation of short DNA fragments, i.e., to an unstable nucleosome structure and decreased nucleosome occupancy at enhancers.

To test whether H2A.Z deposition affects chromatin accessibility, we treated the control and H2A.Z knockdown cells with Benzonase (the nuclease from *Serratia marcescens*) followed by deep sequencing of chromatin cleavage sites (BNase-seq). This approach is similar to DNase-seq but has the advantage of being less sensitive to enzyme concentration (Grøntved et al., 2012). The BNase cleavage sites were highly enriched immediately upstream of TSS and in linker regions (Figure 3C). The BNase-seq tag density was positively correlated with gene expression levels at promoters and with H3K27ac levels at enhancers (Figure 3D), indicating that cleavage by Benzonase is a good indicator of chromatin accessibility. Moreover, intergenic regions more accessible to Benzonase were associated with higher levels of H2A.Z acetylation and H3K4me3 and with lower levels of H3K27me3 (Figure S3B). Interestingly, knockdown of H2A.Z resulted in significantly decreased chromatin accessibility at a subset of genomic regions, as exemplified by several enhancer regions near *Klf4* and *Tbx3* (Figure 3E, highlighted in red boxes). Globally, we found that 19.4% of Benzonase hypersensitive sites showed a significant reduction of BNase cleavage following H2A.Z knockdown, while only 0.7% exhibited increases (Figure 3F). Intriguingly, the regions with lower chromatin accessibility, as measured by the average Benzonase tag density, were subject to greater decreases in chromatin accessibility after knockdown (Figures S3C and S3D). To determine if the reduced chromatin accessibility is correlated with decreased binding of MLL complexes, we monitored RbBP5 binding and found that hypersensitive sites with reduced accessibility were subject to greater decreases in RbBP5 binding after the H2A.Z knockdown (Figure S3E). To test whether the decrease in chromatin accessibility is related to changes in gene expression, we identified 2,986 genes with decreased accessibility at hypersensitive sites located ±100 kb around the TSS and compared these with the 1,204 genes with changed expression. The analysis revealed that 205 were shared between the two sets, which is highly significant (binominal test, $p < 0.0001$) (Figure S3F). These 205 genes are enriched in GO terms of system development and embryonic development (Figure S3G).

Overall, these results indicate that deposition of H2A.Z results in an abnormal and unstable nucleosome structure leading to decreased nucleosome occupancy and thereby increasing chromatin accessibility, particularly at enhancers.

H2A.Z Is Required for Efficient Self-Renewal and Pluripotency of ESCs

The observation that H2A.Z is critically involved in modulating nucleosome occupancy and chromatin accessibility at enhancers implies that it plays important roles in ESC function. We therefore investigated whether it contributes to the self-renewal of ESCs using several different assays. (1) By examining ESC colony morphology, we found that only 56% of colonies that grew for 7 days after H2A.Z knockdown (shH2A.Z) exhibited ESC morphology, while 81% of the colonies that grew from the control ESCs (shLuc) maintained ESC morphology (Figures 4A and 4B); (2) H2A.Z knockdown ESC colonies tended to become flat and had lower alkaline phosphatase activity (Figure 4C); (3) flow cytometry analysis revealed that a greater fraction of cells had lower SSEA1 expression after 2 days of H2A.Z knockdown (13.9% in control and 24.5% in knockdown cells) and increased SSEA4 expression (1.3% in control and 14.5% in knockdown cells), although OCT4 expression in the majority of cells did not change much (Figure 4D); (4) knockdown of H2A.Z resulted in substantial decreases in expression of pluripotency genes such as *Sox2*, *Esrrb*, *Tbx3*, and *Klf4* and increases in expression of differentiation genes such as *Brachyury*, *Hand1*, and *Wnt7b* (Figures 4E and S4A). In addition, genes responsive to H2A.Z knockdown in ESCs are enriched in GO terms of system development and embryonic development (Figure S4B). (5) Comparing genes responsive to H2A.Z knockdown in ESCs and those whose expression was altered at embryoid bodies (EBs) on day 3 during EB formation revealed a highly significant overlap between the two groups (Figure 4F). Overall, these results indicate a loss of pluripotency and self-renewal capacity of ESCs after knockdown of H2A.Z, accompanied by premature differentiation. Thus H2A.Z critically contributes to the self-renewal and pluripotency of ESCs as well as to their differentiation.

H2A.Z Facilitates Targeting of OCT4 to Genes Critical to ESC Pluripotency

To understand the mechanisms whereby H2A.Z contributes to the self-renewal of ESCs, we tested whether H2A.Z regulates targeting of the transcription factor OCT4. Using ChIP-seq, we identified genome-wide OCT4 binding sites in the H2A.Z knockdown and control ESCs. Analysis indicated that H2A.Z binding is highly elevated at OCT4 binding sites in control ESCs (Figure 5A). Knockdown of H2A.Z leads to substantially

(C) H2A.Z knockdown (shH2A.Z) and shLuc control ESCs stained for alkaline phosphatase activity.

(D) FACS analysis showing the distribution of expression of SSEA-1 (a pluripotency marker for murine ESCs) and SSEA-4 (a differentiation marker for murine ESCs) relative to OCT4 (a pluripotency transcription factor) for ESCs with H2A.Z knockdown (shH2A.Z) and shLuc control cells. The analysis was done after 2 days of culture following replating from individual ESC colonies.

(E) RT-PCR results (averages of three replicates) for mRNAs of four pluripotency genes and two early differentiation markers in the H2A.Z knockdown (shH2A.Z) and shLuc control ESCs. Data are represented as mean ± SD.

(F) Venn diagrams for genes responsive to H2A.Z knockdown in ESCs (up- or downregulated by more than 1.5-fold and FDR < 0.001; left circles) and genes that are up- or downregulated during EB formation from ESCs to EB day 3 (EB-associated genes; right circles). See also Figure S4.

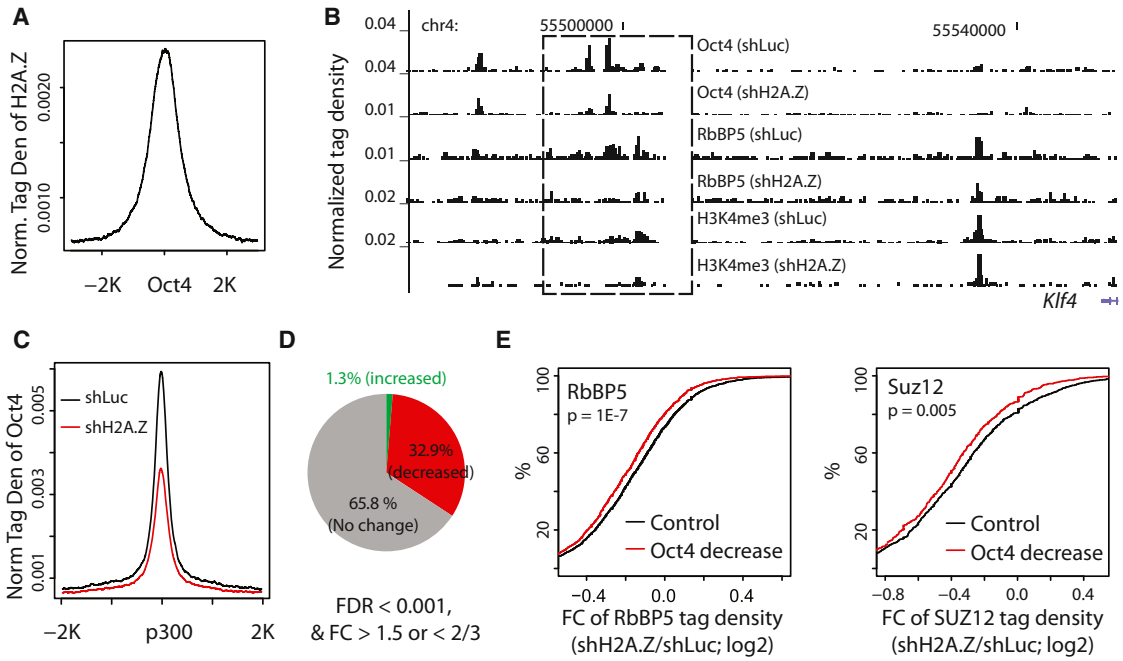

Figure 5. H2A.Z Is Required for Efficient Binding of OCT4

(A) Average profile of H2A.Z tag density around OCT4 binding sites in mouse ESCs.

(B) UCSC Genome Browser image of tag distribution of OCT4, RbBP5, and H3K4me3 in the putative enhancer regions downstream of the *Klf4* gene in control and H2A.Z knockdown ESCs. The genomic region that shows significant decreases in the levels of Oct4, RbBP5, and H3K4me3 is highlighted by the rectangle.

(C) Average profile of OCT4 tag density around intergenic p300 binding sites in the H2A.Z knockdown (shH2A.Z) and control (shLuc) ES cells.

(D) The percentages of OCT4 binding sites that showed a significant increase (green), decrease (red), or no change (gray) after knockdown of H2A.Z.

(E) Left panel: intergenic OCT4 binding sites that colocalize with RbBP5 are separated into two groups based on whether or not OCT4 binding is significantly decreased upon H2A.Z knockdown (FC > 1.5, FDR < 0.001). The empirical cumulative distribution is plotted for the FC of RbBP5 ChIP-seq tag density for each group (knockdown/control). Right panel: same as the left panel, except the calculation was made for SUZ12 (x axis). A line shifting to the left means a greater decrease in RbBP5 (or SUZ12) binding levels. p values were calculated by Kolmogorov-Smirnov tests.

decreased OCT4 binding at several putative enhancers downstream of the *Klf4* gene (Figure 5B), accompanied by decreased expression of the *Klf4* gene (Figure 4E). Furthermore, H2A.Z knockdown resulted in a global decrease of OCT4 binding at p300-bound enhancers (Figure 5C), though the overall expression level of OCT4 itself was not significantly affected (Figure 4E). Quantitative analysis indicated that 33% of OCT4 binding sites showed decreased binding after H2A.Z knockdown, while only 1.3% showed increased binding (Figure 5D). Since OCT4 may directly interact with MLL complexes (Ang et al., 2011), reduced OCT4 binding after H2A.Z knockdown may compromise the recruitment of MLL complexes and thus H3K4 methylation. Indeed, upon knockdown of H2A.Z and loss of OCT4 binding, RbBP5 binding and H3K4me3 levels at the *Klf4* enhancer regions markedly decreased (Figure 5B). Globally, a significantly larger RbBP5 loss was detected at enhancer sites that lost OCT4 binding than at sites that did not lose OCT4 (Figure 5E, left panel).

H2A.Z also plays an important role in the establishment of the H3K27me3 modification and SUZ12 binding in the repression of differentiation genes, as seen from the results of H2A.Z knockdown in Figures 2A, 2B, and 4E. Interestingly, the loss of SUZ12 at enhancers after H2A.Z knockdown was also significantly related to a decreased binding of OCT4 (Figure 5E, right panel).

These results indicate that H2A.Z is needed for efficient targeting of OCT4, which is likely involved in the recruitment of the MLL and PRC2 complexes to active and silent genes, respectively.

H2A.Z Is Required for Efficient Differentiation of ESCs

The results in Figure 4 indicate that ESCs with reduced H2A.Z expression tend to differentiate. To further test whether knockdown of H2A.Z promotes ESC differentiation, we monitored the formation of EBs from control and H2A.Z knockdown ESCs. The EBs from the H2A.Z knockdown cells were morphologically different from the control ESCs: although a primitive endoderm layer from control cells formed at day 4, this layer was not detectable in the knockdown cells at day 4 and only became apparent at day 7 (Figure 6A, red arrow heads). RT-PCR analyses showed that H2A.Z remained suppressed during the period of 14 day differentiation in the knockdown cells (Figure 6B). In the knockdown cells (shH2A.Z), the expression of pluripotency genes *Nanog*, *Oct4*, and *Klf4* is somewhat compromised at day 1 of differentiation, but they remain active at 14 days in contrast to the control cells (shLuc) (Figure 6B, inserts). Consistent with delayed endodermal differentiation phenotypes, knockdown of H2A.Z resulted in decreased induction of a number of endodermal transcription factors (*Gata6*, *Hnf1b*, and *Hnf4a*), markers of visceral endoderm (*Afp*, *Ttr*, and

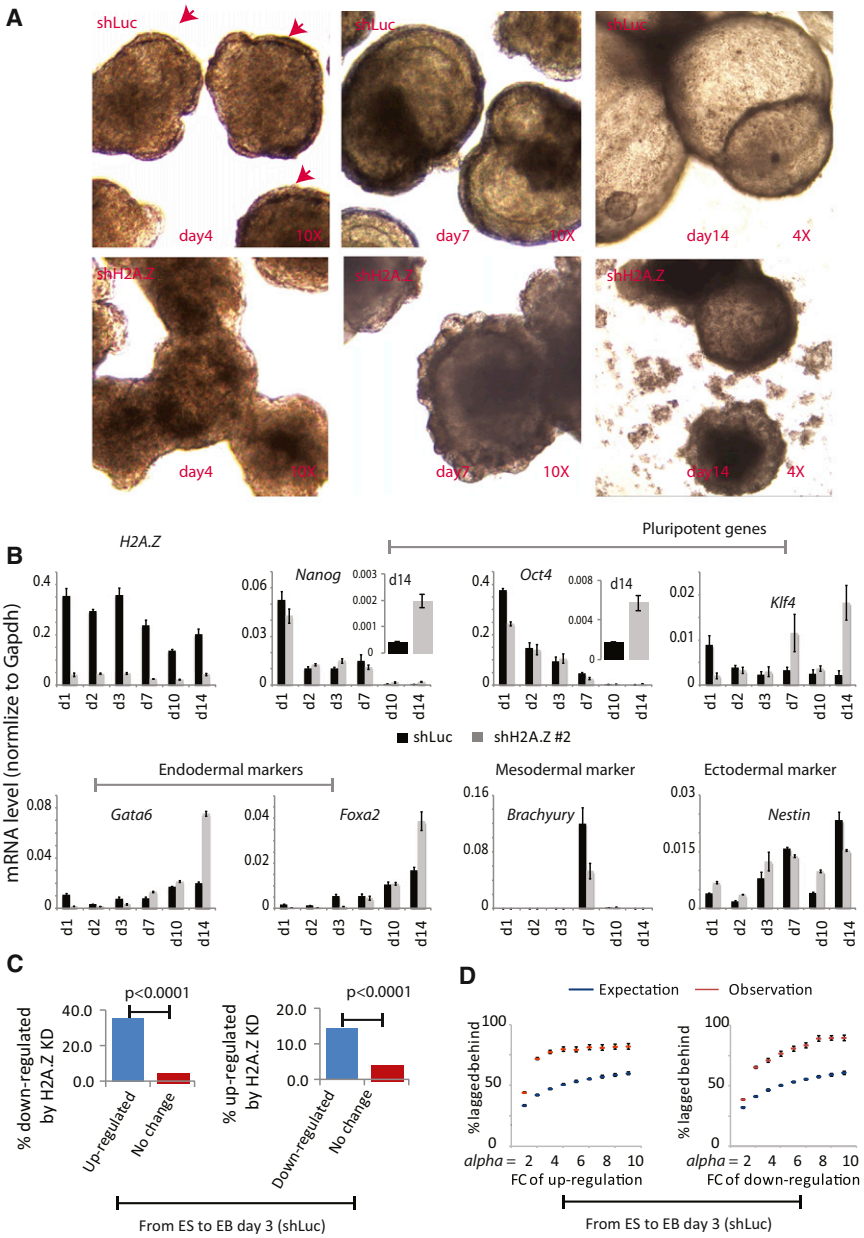

Figure 6. H2A.Z Is Required for Efficient Differentiation of ESCs

(A) Comparative morphology of H2A.Z knockdown (shH2A.Z) and control (shLuc) EBs at day 4, day 7, and day 14. Primitive endoderm layers are indicated by red arrows.

(B) RT-PCR results for mRNAs from the H2A.Z knockdown (shH2A.Z) and shLuc (control) EBs. Data are represented as mean ± SD.

(C) Left panel: the percentage of genes downregulated by H2A.Z knockdown at EB day 3 (y axis) plotted for genes that are significantly upregulated (blue) and unchanged (red) in transition from WT ESCs to EB day 3. Right panel: the percentage of genes upregulated by H2A.Z knockdown at EB day 3 (y axis) plotted for genes that are significantly downregulated (blue) and unchanged (red) from WT ESCs to EB day 3. p values were calculated by the t test.

(D) Left panel: each point represents genes upregulated by at least alpha-fold from ESCs to EB day 3 in the control cells. The percentage of genes with expression values that follow the order EB day 3 (shLuc) > EB day 3 (shH2A.Z) > ESCs is calculated for each point (y axis). The expression values of all genes are randomly shuffled independently for EB day 3 (shLuc), EB day 3 (shH2A.Z), and ESCs and are repeated many times to estimate the expected percentage. Right panel: similar to the left panel but for genes that are downregulated by at least alpha-fold from ESCs to EB day 3 in the control cells. The y axis shows the percentage of genes with expression levels following the order EB day 3 (shLuc) < EB day 3 (shH2A.Z) < ESCs. Data are represented as mean ± SD. See also Figure S5.

Bmp2), and parietal endoderm (*Dab2*) at day 3 and to a lesser extent at day 7 (Figures 6B, S5A, and S5B). In addition, mesodermal markers *Brachyury*, *Hand1*, *Nkx2-5*, *Bmp4*, and *Runx1* and ectodermal markers *Sox4* and *Nestin* were aberrantly expressed but showed no generalizable pattern of consistent up- or downregulation (Figures 6B, S5A, and S5B). These results indicate that knockdown of H2A.Z compromised both gene activation and repression in EB formation.

To test this notion systematically, we identified genes that are activated or repressed in day 3 EBs as compared to ESCs and then noted the proportion of these two groups of genes that failed to be efficiently activated or repressed in the H2A.Z knockdown EBs; this was 35.5% of the activated and 14.4% of the repressed genes, which is significantly higher than the number of genes that remained unchanged during EB formation (Figure 6C). This shows that during EB formation, changes in gene expression are generally less in the H2A.Z knockdown cells than in the control cells; i.e., H2A.Z knockdown compromises both the activation of genes required for EB development and the repression of genes required for pluripotency. To test this rigorously, we first identified genes that are upregulated during EB formation from control ESCs to day 3 and calculated the fraction of these genes that exhibited a lower induction level in the H2A.Z knockdown EBs as compared to the control EBs. We found that this fraction is significantly higher than expected (Figure 6D, left), indicating that knockdown of H2A.Z compromised the induction of these genes. Similarly, knockdown of H2A.Z also compromised the repression of genes during EB formation (Figure 6D, right).The defect in gene upregulation was particularly significant for endodermal markers at day 3 (Figure S5A), which is consistent with the defect in endodermal phenotype shown in Figure 6A.

In conclusion, although knockdown of H2A.Z leads to decreased expression of many pluripotency genes and upregulation of differentiation genes, it is also required for the silencing of ESC-specific genes and the optimal activation of differentiation genes during differentiation of ESCs.

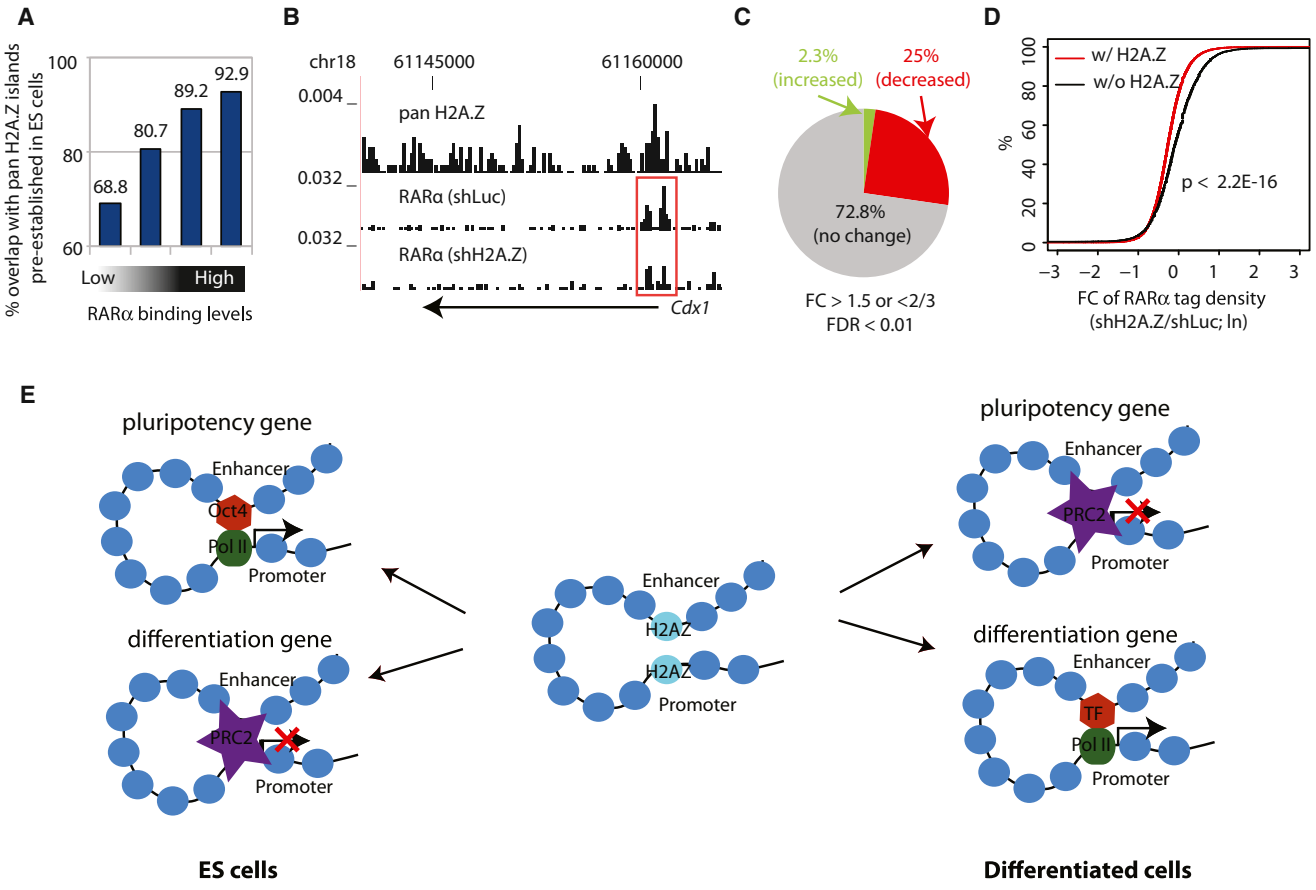

Figure 7. H2A.Z Facilitates RARα Binding during RA-Induced ESC Differentiation

(A) RARα bound genomic regions were sorted into quartiles based on RARα enrichment levels after 3 hr of RA exposure. The y axis indicates the percentage of RARα bound regions that overlap with pan H2A.Z islands identified in ESCs.

(B) UCSC Genome Browser image of tag distributions of pan H2A.Z in ESCs and RARα in H2A.Z knockdown (shH2A.Z) and control (shLuc) cells 3 hr after RA exposure for a known RAR target gene *cdx1*. The promoter region that shows a significant decrease in RARα binding is highlighted by the red rectangle.

(C) The percentages of RARα binding sites that showed a significant increase (green), decrease (red), or no change (gray) in RARα binding after knockdown of H2A.Z.

(D) RARα binding sites are separated into two groups according to their association with H2A.Z in the ESCs: the red and black lines represent the RARα binding sites associated with (w/) or without (w/o) H2A.Z, respectively, before the treatment with retinoic acid. The empirical cumulative distribution is plotted for the FC of RARα ChIP-seq tag density for each group (shH2A.Z/shLuc). A line shifting to the left means a systematically larger decrease in the RARα levels. The p value was calculated by Kolmogorov-Smirnov test.

(E) Differential roles of H2A.Z in active and repressed genes in the self-renewal and differentiation of ESCs (see Discussion for details).

H2A.Z Is Required for Efficient Binding of RARα Following Retinoic Acid Treatment

To test whether H2A.Z facilitates transcription factor binding during ESC differentiation, we analyzed the binding profiles of RARα following withdrawal of leukemia inhibitory factor (LIF) and addition of retinoic acid (RA) to ESCs, which initiates ESC differentiation to the neuronal lineage (Diez del Corral and Storey, 2004). Interestingly, a vast majority of the genomic regions bound by RARα after RA exposure were enriched with H2A.Z in ESCs (Figures 7A and 7B), indicating that the chromatin of many developmental enhancers is preconfigured by H2A.Z at earlier stages of development (Amat and Gudas, 2011). Although RARα expression was not affected by H2A.Z knockdown, the binding of RARα was significantly compromised genome-wide: 25% of its bindings showed a decrease, while only 2% showed an increase in knockdown of H2A.Z (Figure 7C). Remarkably, the RARα binding sites preconfigured with H2A.Z in ESCs exhibited more of a decrease in RARα binding than the sites without H2A.Z (Figure 7D), suggesting that setting a chromatin configuration by H2A.Z in ESCs facilitates transcription factor binding during later development.

DISCUSSION

How Does H2A.Z Contribute to the Regulation of Transcription?

Similar to differentiated cells (Barski et al., 2007; Bruce et al., 2005; Cui et al., 2009; Jin et al., 2009), we found that H2A.Z is linked to gene activation in murine ESCs, and its acetylation state correlates with the level of gene expression. H2A.Z colocalizes with H3K4me3 in transcriptional regulatory regions including promoters and enhancers. While this manuscript was being

revised, the colocalization of H2A.Z with H3K4me3 in mouse ESCs was also reported by Ku et al. (2012) who also noted the relationship between its state of acetylation and the level of gene expression. The H2A.Z level at enhancers is positively correlated with H3K27ac, a mark of enhancer activity (Hawkins et al., 2011; Creyghton et al., 2010; Rada-Iglesias et al., 2011), suggesting that it also influences the activity of enhancers. Incorporation of H2A.Z into nucleosomes leads to an unstable structure in vitro (Jin et al., 2009). Furthermore, it was recently shown that H2A.Z deposition at promoter regions facilitates gene activation following 5-Aza-CdR-induced demethylation in cancer cells; this is achieved by a reduction of nucleosome occupancy and generating a permissive environment (Yang et al., 2012). Consistent with these observations, inclusion of H2A.Z generates an abnormal nucleosome and protects only 120 bp of DNA from MNase digestion in T cells (Tolstorukov et al., 2009). Thus H2A.Z appears to regulate chromatin accessibility by modulating nucleosome occupancy at regulatory regions. Indeed, our data indicate that knocking down H2A.Z in murine ESCs leads to a decrease in the number of smaller H2A.Z nucleosomes and an increase in general nucleosome occupancy at critical *cis*-regulatory regions. Consistent with these results, knockdown of H2A.Z results in decreased chromatin accessibility when probed by Benzonase digestion. These results support the hypothesis that H2A.Z is an essential component of an unstable nucleosome, from which the octamer can readily be evicted or displaced, as described earlier (Jin et al., 2009). The loss or displacement of nucleosomes from DNA allows the binding of factors/complexes at various *cis* elements where H2A.Z is found including transcription complexes at active TSS, PRC2 at bivalent TSS, and sequence-specific transcription factors at enhancers. H2A.Z therefore appears as a general facilitator for the activity of a wide variety of other functional factors/complexes.

How Does H2A.Z Contribute to the Self-Renewal and Differentiation of ESCs?

We demonstrate that H2A.Z is required for efficient self-renewal of ESCs. In the H2A.Z knockdown cells, expression of many transcription factors critical for ESC function such as *Klf4*, *Tbx3*, and *Sox2* was decreased. It has previously been shown that the pluripotency transcription factor, OCT4, binds to enhancers and mediates activation of characteristic ESC genes. OCT4 binding could directly promote the assembly of the transcription machinery or promote H3K4 methylation by recruiting the MLL complexes (Ang et al., 2011). Our data indicate that H2A.Z-mediated chromatin accessibility is critical for OCT4 targeting to enhancers; knockdown of H2A.Z compromises OCT4 binding to the downstream enhancers of the *Klf4* gene. At a global level, inhibition of H2A.Z decreased OCT4 binding over a large fraction of its target sites, which leads to less efficient recruitment of MLL complexes, decreased H3K4 methylation, and downregulation of key ESC genes.

Inhibition of H2A.Z also led to increased expression of differentiation genes in ESCs. Others have shown (Creyghton et al., 2008), and we confirm here, that reduction of H2A.Z compromises targeting of the PRC2 complex and decreases H3K27 trimethylation, resulting in activation of differentiation genes normally repressed in ESCs. Our data suggest that H2A.Z-mediated OCT4 targeting might also be involved in recruitment of SUZ12 to a subset of the repressed enhancers.

Although inhibition of H2A.Z triggers premature differentiation of ESCs, H2A.Z is required for efficient ESC differentiation. Similar to the self-renewal of ESCs, the chromatin accessibility mediated by deposition of H2A.Z may be critical for full activation of differentiation genes and complete repression of ESC-specific genes during differentiation of ESCs. Indeed, we observed that both gene activation and repression during EB formation were compromised on H2A.Z knockdown. Furthermore, we find that preconfiguration of chromatin by H2A.Z is required for optimal targeting of RARα during RA-induced differentiation of ESCs.

In summary, we provide data showing differential roles of H2A.Z at active and repressed genes in the self-renewal and differentiation of ESCs (Figure 7E). H2A.Z facilitates expression of many pluripotency genes and also the repression of differentiation genes by generating chromatin accessibility and thereby facilitating the efficient targeting of activating and repressive complexes, respectively. During differentiation of ESCs, optimal induction of differentiation genes and the complete silencing of pluripotency genes also require H2A.Z to facilitate access of the appropriate complexes. For these reasons we propose that H2A.Z is a general facilitator that generates access for a wide variety of activating and repressive complexes.

EXPERIMENTAL PROCEDURES

Cells and Cell Culture

CMTi and R1 murine ESC lines were routinely cultured on feeder-coated dishes in ESC-qualified Dulbecco's modified Eagle's medium (DMEM) supplemented with various growth factors. More details and analysis of ESC morphology, EB formation, and RA treatment are described in Supplemental Experimental Procedures.

Knockdown of H2A.Z and MLL4 Using shRNA

The RNA interference constructs targeting mouse H2A.Z and MLL4 were generated by inserting target sequences (Supplemental Experimental Procedures) into pGreenPuro Lentivector (System Biosciences). The lentiviral particles were packaged in 293T cells with the psPAX2 packaging plasmid, and lentiviral supernatants were then used to infect mouse ESCs for knockdown experiments.

Chromatin Preparation, Antibodies, and ChIP-Seq

ChIP-seq experiments were performed as described previously (Barski et al., 2007) with antibodies against pan H2A.Z and acH2A.Z (Bruce et al., 2005). Other antibodies used in ChIP-seq experiments of this study are listed in Table S1.

BNase-Seq for Chromatin Accessibility Assay

The method of Benzonase digestion for a genome-wide profiling of chromatin accessibility followed that described by Grøntved et al. (2012) with some modifications (Supplemental Experimental Procedures).

Public ChIP-Seq Data

Other ChIP-seq data obtained from the GEO database for mouse ESCs include H3K27ac, H3K4me3, H3K27me3, H3K36me3, and p300 (Creyghton et al., 2010; Mikkelsen et al., 2007).

Data Analysis

Sequence alignment and peak calling, definition of genomic regions, heatmaps for the distribution of histone modifications at promoters and enhancers, Pearson coefficients for similarity of spatial distributions between two epigenetic markers, MA analysis, and definition of differentially expressed genes are described in Supplemental Experimental Procedures.

ACCESSION NUMBERS

The GEO accession number for data reported in this paper is GSE34483.

SUPPLEMENTAL INFORMATION

Supplemental Information includes five figures, one table, and Supplemental Experimental Procedures and can be found with this article online at http://dx.doi.org/10.1016/j.stem.2012.11.003.

ACKNOWLEDGMENTS

We thank Zhibin Wang, Dustin E. Schones, Iouri Chepelev, Brian J. Abraham, Gang Wei, Daniel Kraushaar, and Benjamin Kidder for helpful discussions. The DNA Sequencing Core and the Flow Cytometry Core of the National Institute of Heart, Lung, and Blood Institute (NHLBI) assisted with this work. Support was provided by the Division of Intramural Research Program of the NHLBI, NIH.

Received: May 9, 2012
Revised: September 29, 2012
Accepted: November 8, 2012
Published: December 20, 2012

REFERENCES

Amat, R., and Gudas, L.J. (2011). RARγ is required for correct deposition and removal of Suz12 and H2A.Z in embryonic stem cells. J. Cell. Physiol. *226*, 293–298.

Ang, Y.S., Tsai, S.Y., Lee, D.F., Monk, J., Su, J., Ratnakumar, K., Ding, J., Ge, Y., Darr, H., Chang, B., et al. (2011). Wdr5 mediates self-renewal and reprogramming via the embryonic stem cell core transcriptional network. Cell *145*, 183–197.

Barski, A., Cuddapah, S., Cui, K., Roh, T.Y., Schones, D.E., Wang, Z., Wei, G., Chepelev, I., and Zhao, K. (2007). High-resolution profiling of histone methylations in the human genome. Cell *129*, 823–837.

Bruce, K., Myers, F.A., Mantouvalou, E., Lefevre, P., Greaves, I., Bonifer, C., Tremethick, D.J., Thorne, A.W., and Crane-Robinson, C. (2005). The replacement histone H2A.Z in a hyperacetylated form is a feature of active genes in the chicken. Nucleic Acids Res. *33*, 5633–5639.

Cao, R., and Zhang, Y. (2004). SUZ12 is required for both the histone methyltransferase activity and the silencing function of the EED-EZH2 complex. Mol. Cell *15*, 57–67.

Cho, Y.W., Hong, T., Hong, S., Guo, H., Yu, H., Kim, D., Guszczynski, T., Dressler, G.R., Copeland, T.D., Kalkum, M., and Ge, K. (2007). PTIP associates with MLL3- and MLL4-containing histone H3 lysine 4 methyltransferase complex. J. Biol. Chem. *282*, 20395–20406.

Cho, Y.W., Hong, S., Jin, Q., Wang, L., Lee, J.E., Gavrilova, O., and Ge, K. (2009). Histone methylation regulator PTIP is required for PPARgamma and C/EBPalpha expression and adipogenesis. Cell Metab. *10*, 27–39.

Conerly, M.L., Teves, S.S., Diolaiti, D., Ulrich, M., Eisenman, R.N., and Henikoff, S. (2010). Changes in H2A.Z occupancy and DNA methylation during B-cell lymphomagenesis. Genome Res. *20*, 1383–1390.

Creyghton, M.P., Markoulaki, S., Levine, S.S., Hanna, J., Lodato, M.A., Sha, K., Young, R.A., Jaenisch, R., and Boyer, L.A. (2008). H2AZ is enriched at polycomb complex target genes in ES cells and is necessary for lineage commitment. Cell *135*, 649–661.

Creyghton, M.P., Cheng, A.W., Welstead, G.G., Kooistra, T., Carey, B.W., Steine, E.J., Hanna, J., Lodato, M.A., Frampton, G.M., Sharp, P.A., et al. (2010). Histone H3K27ac separates active from poised enhancers and predicts developmental state. Proc. Natl. Acad. Sci. USA *107*, 21931–21936.

Cui, K., Zang, C., Roh, T.Y., Schones, D.E., Childs, R.W., Peng, W., and Zhao, K. (2009). Chromatin signatures in multipotent human hematopoietic stem cells indicate the fate of bivalent genes during differentiation. Cell Stem Cell *4*, 80–93.

Diez del Corral, R., and Storey, K.G. (2004). Opposing FGF and retinoid pathways: a signalling switch that controls differentiation and patterning onset in the extending vertebrate body axis. Bioessays *26*, 857–869.

Dou, Y., Milne, T.A., Ruthenburg, A.J., Lee, S., Lee, J.W., Verdine, G.L., Allis, C.D., and Roeder, R.G. (2006). Regulation of MLL1 H3K4 methyltransferase activity by its core components. Nat. Struct. Mol. Biol. *13*, 713–719.

Dryhurst, D., Ishibashi, T., Rose, K.L., Eirín-López, J.M., McDonald, D., Silva-Moreno, B., Veldhoen, N., Helbing, C.C., Hendzel, M.J., Shabanowitz, J., et al. (2009). Characterization of the histone H2A.Z-1 and H2A.Z-2 isoforms in vertebrates. BMC Biol. *7*, 86.

Ernst, J., Kheradpour, P., Mikkelsen, T.S., Shoresh, N., Ward, L.D., Epstein, C.B., Zhang, X., Wang, L., Issner, R., Coyne, M., et al. (2011). Mapping and analysis of chromatin state dynamics in nine human cell types. Nature *473*, 43–49.

Fan, J.Y., Gordon, F., Luger, K., Hansen, J.C., and Tremethick, D.J. (2002). The essential histone variant H2A.Z regulates the equilibrium between different chromatin conformational states. Nat. Struct. Biol. *9*, 172–176.

Fan, J.Y., Rangasamy, D., Luger, K., and Tremethick, D.J. (2004). H2A.Z alters the nucleosome surface to promote HP1alpha-mediated chromatin fiber folding. Mol. Cell *16*, 655–661.

Goldberg, A.D., Banaszynski, L.A., Noh, K.M., Lewis, P.W., Elsaesser, S.J., Stadler, S., Dewell, S., Law, M., Guo, X., Li, X., et al. (2010). Distinct factors control histone variant H3.3 localization at specific genomic regions. Cell *140*, 678–691.

Goldman, J.A., Garlick, J.D., and Kingston, R.E. (2010). Chromatin remodeling by imitation switch (ISWI) class ATP-dependent remodelers is stimulated by histone variant H2A.Z. J. Biol. Chem. *285*, 4645–4651.

Grøntved, L., Bandle, R., John, S., Baek, S., Chung, H.J., Liu, Y., Aguilera, G., Oberholtzer, C., Hager, G.L., and Levens, D. (2012). Rapid genome-scale mapping of chromatin accessibility in tissue. Epigenetics Chromatin *5*, 10.

Guenther, M.G., Levine, S.S., Boyer, L.A., Jaenisch, R., and Young, R.A. (2007). A chromatin landmark and transcription initiation at most promoters in human cells. Cell *130*, 77–88.

Hardy, S., Jacques, P.E., Gévry, N., Forest, A., Fortin, M.E., Laflamme, L., Gaudreau, L., and Robert, F. (2009). The euchromatic and heterochromatic landscapes are shaped by antagonizing effects of transcription on H2A.Z deposition. PLoS Genet. *5*, e1000687.

Hawkins, R.D., Hon, G.C., Yang, C., Antosiewicz-Bourget, J.E., Lee, L.K., Ngo, Q.M., Klugman, S., Ching, K.A., Edsall, L.E., Ye, Z., et al. (2011). Dynamic chromatin states in human ES cells reveal potential regulatory sequences and genes involved in pluripotency. Cell Res. *21*, 1393–1409.

He, H.H., Meyer, C.A., Shin, H., Bailey, S.T., Wei, G., Wang, Q., Zhang, Y., Xu, K., Ni, M., Lupien, M., et al. (2010). Nucleosome dynamics define transcriptional enhancers. Nat. Genet. *42*, 343–347.

Heintzman, N.D., Stuart, R.K., Hon, G., Fu, Y., Ching, C.W., Hawkins, R.D., Barrera, L.O., Van Calcar, S., Qu, C., Ching, K.A., et al. (2007). Distinct and predictive chromatin signatures of transcriptional promoters and enhancers in the human genome. Nat. Genet. *39*, 311–318.

Hu, G., Schones, D.E., Cui, K., Ybarra, R., Northrup, D., Tang, Q., Gattinoni, L., Restifo, N.P., Huang, S., and Zhao, K. (2011). Regulation of nucleosome landscape and transcription factor targeting at tissue-specific enhancers by BRG1. Genome Res. *21*, 1650–1658.

Jin, C.Y., and Felsenfeld, G. (2007). Nucleosome stability mediated by histone variants H3.3 and H2A.Z. Genes Dev. *21*, 1519–1529.

Jin, C.Y., Zang, C.Z., Wei, G., Cui, K.R., Peng, W.Q., Zhao, K.J., and Felsenfeld, G. (2009). H3.3/H2A.Z double variant-containing nucleosomes mark 'nucleosome-free regions' of active promoters and other regulatory regions. Nat. Genet. *41*, 941–945.

Kim, T.H., Barrera, L.O., Zheng, M., Qu, C., Singer, M.A., Richmond, T.A., Wu, Y., Green, R.D., and Ren, B. (2005). A high-resolution map of active promoters in the human genome. Nature *436*, 876–880.

Kim, H.S., Vanoosthuyse, V., Fillingham, J., Roguev, A., Watt, S., Kislinger, T., Treyer, A., Carpenter, L.R., Bennett, C.S., Emili, A., et al. (2009). An

acetylated form of histone H2A.Z regulates chromosome architecture in Schizosaccharomyces pombe. Nat. Struct. Mol. Biol. *16*, 1286–1293.

Ku, M., Jaffe, J.D., Koche, R.P., Rheinbay, E., Endoh, M., Koseki, H., Carr, S.A., and Bernstein, B.E. (2012). H2A.Z landscapes and dual modifications in pluripotent and multipotent stem cells underlie complex genome regulatory functions. Genome Biol. *13*, R85.

Leach, T.J., Mazzeo, M., Chotkowski, H.L., Madigan, J.P., Wotring, M.G., and Glaser, R.L. (2000). Histone H2A.Z is widely but nonrandomly distributed in chromosomes of Drosophila melanogaster. J. Biol. Chem. *275*, 23267–23272.

Meissner, A., Mikkelsen, T.S., Gu, H.C., Wernig, M., Hanna, J., Sivachenko, A., Zhang, X.L., Bernstein, B.E., Nusbaum, C., Jaffe, D.B., et al. (2008). Genome-scale DNA methylation maps of pluripotent and differentiated cells. Nature *454*, 766–770.

Mikkelsen, T.S., Ku, M.C., Jaffe, D.B., Issac, B., Lieberman, E., Giannoukos, G., Alvarez, P., Brockman, W., Kim, T.K., Koche, R.P., et al. (2007). Genome-wide maps of chromatin state in pluripotent and lineage-committed cells. Nature *448*, 553–560.

Pekowska, A., Benoukraf, T., Ferrier, P., and Spicuglia, S. (2010). A unique H3K4me2 profile marks tissue-specific gene regulation. Genome Res. *20*, 1493–1502.

Pekowska, A., Benoukraf, T., Zacarias-Cabeza, J., Belhocine, M., Koch, F., Holota, H., Imbert, J., Andrau, J.C., Ferrier, P., and Spicuglia, S. (2011). H3K4 tri-methylation provides an epigenetic signature of active enhancers. EMBO J. *30*, 4198–4210.

Rada-Iglesias, A., Bajpai, R., Swigut, T., Brugmann, S.A., Flynn, R.A., and Wysocka, J. (2011). A unique chromatin signature uncovers early developmental enhancers in humans. Nature *470*, 279–283.

Rangasamy, D., Berven, L., Ridgway, P., and Tremethick, D.J. (2003). Pericentric heterochromatin becomes enriched with H2A.Z during early mammalian development. EMBO J. *22*, 1599–1607.

Ren, Q.H., and Gorovsky, M.A. (2001). Histone H2A.Z acetylation modulates an essential charge patch. Mol. Cell *7*, 1329–1335.

Roh, T.Y., Cuddapah, S., and Zhao, K. (2005). Active chromatin domains are defined by acetylation islands revealed by genome-wide mapping. Genes Dev. *19*, 542–552.

Roh, T.Y., Wei, G., Farrell, C.M., and Zhao, K. (2007). Genome-wide prediction of conserved and nonconserved enhancers by histone acetylation patterns. Genome Res. *17*, 74–81.

Schones, D.E., Cui, K.R., Cuddapah, S., Roh, T.Y., Barski, A., Wang, Z.B., Wei, G., and Zhao, K.J. (2008). Dynamic regulation of nucleosome positioning in the human genome. Cell *132*, 887–898.

Schuettengruber, B., Chourrout, D., Vervoort, M., Leblanc, B., and Cavalli, G. (2007). Genome regulation by polycomb and trithorax proteins. Cell *128*, 735–745.

Thambirajah, A.A., Dryhurst, D., Ishibashi, T., Li, A., Maffey, A.H., and Ausió, J. (2006). H2A.Z stabilizes chromatin in a way that is dependent on core histone acetylation. J. Biol. Chem. *281*, 20036–20044.

Tillo, D., Kaplan, N., Moore, I.K., Fondufe-Mittendorf, Y., Gossett, A.J., Field, Y., Lieb, J.D., Widom, J., Segal, E., and Hughes, T.R. (2010). High nucleosome occupancy is encoded at human regulatory sequences. PLoS ONE *5*, e9129.

Tolstorukov, M.Y., Kharchenko, P.V., Goldman, J.A., Kingston, R.E., and Park, P.J. (2009). Comparative analysis of H2A.Z nucleosome organization in the human and yeast genomes. Genome Res. *19*, 967–977.

Valdés-Mora, F., Song, J.Z., Statham, A.L., Strbenac, D., Robinson, M.D., Nair, S.S., Patterson, K.I., Tremethick, D.J., Stirzaker, C., and Clark, S.J. (2012). Acetylation of H2A.Z is a key epigenetic modification associated with gene deregulation and epigenetic remodeling in cancer. Genome Res. *22*, 307–321. . Published online July 25, 2011.

Wang, Z.B., Zang, C.Z., Rosenfeld, J.A., Schones, D.E., Barski, A., Cuddapah, S., Cui, K.R., Roh, T.Y., Peng, W.Q., Zhang, M.Q., and Zhao, K. (2008). Combinatorial patterns of histone acetylations and methylations in the human genome. Nat. Genet. *40*, 897–903.

Yang, X., Noushmehr, H., Han, H., Andreu-Vieyra, C., Liang, G., and Jones, P.A. (2012). Gene reactivation by 5-aza-2′-deoxycytidine-induced demethylation requires SRCAP-mediated H2A.Z insertion to establish nucleosome depleted regions. PLoS Genet. *8*, e1002604.

Zang, C.Z., Schones, D.E., Zeng, C., Cui, K.R., Zhao, K.J., and Peng, W.Q. (2009). A clustering approach for identification of enriched domains from histone modification ChIP-Seq data. Bioinformatics *25*, 1952–1958.

Zilberman, D., Coleman-Derr, D., Ballinger, T., and Henikoff, S. (2008). Histone H2A.Z and DNA methylation are mutually antagonistic chromatin marks. Nature *456*, 125–129.

Zlatanova, J., and Thakar, A. (2008). H2A.Z: view from the top. Structure *16*, 166–179.